Heliyon 10 (2024) e30287

Contents lists available at ScienceDirect

Heliyon

journal homepage: www.cell.com/heliyon

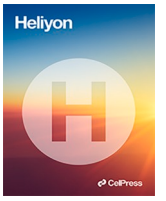

Research article

Identification of potent inhibitors of kynurenine-3-monooxygenase from natural products: *In silico and in vitro* approaches

Redouane Rebai [a,e,*], Miguel Carmena-Bargueño [b], Mohammed Esseddik Toumi [c], Imene Derardja [a], Luc Jasmin [d], Horacio Pérez-Sánchez [b], Abdennacer Boudah [e]

[a] *Department of Natural and Life Sciences, University Mohamed Khider of Biskra, BP 145 RP, 07000, Biskra, Algeria*
[b] *Structural Bioinformatics and High-Performance Computing Research Group (BIO-HPC), Computer Engineering Department, Universidad Católica de Murcia (UCAM), Campus de los Jerónimos 135, 30107, Guadalupe, Spain*
[c] *Laboratory of Microbiological Engineering and Application, Biochemistry and Molecular and Cellular Biology Department, Faculty of Nature and Life Sciences, University of Mentouri Brothers Constantine 1, Constantine, 25017, Algeria*
[d] *Department of Oral and Maxillofacial Surgery, University of California, San Francisco, 707 Parnassus Ave Suite D-1201, San Francisco, CA, 94143, USA*
[e] *Laboratory of biotechnology, National Higher School of Biotechnology, Ville universitaire (university of Constantine 3) Ali Mendjeli, BP E66 25100, Constantine, Algeria*

ARTICLE INFO

Keywords:
Molecular docking
Molecular dynamics
Kinetic assays
Flavonoids
KMO inhibition

ABSTRACT

Existing inhibitors of kynurenine-3-monooxygenase (KMO) have side effects and poorly cross the blood-brain barrier. Therefore, the discovery of new molecules targeting KMO isnecessary.This study aims to develop a novel therapeutic drug targeting KMO using computational methods and experimental validation of natural compounds.The results of our study show that the top four compounds, namely, 3′-Hydroxy-alpha-naphthoflavone exhibited the best docking scores with KMO (−10.0 kcal/mol), followed by 3′-Hydroxy-ss-naphthoflavone (−9.9 kcal/mol), genkwanin (−9.2 kcal/mol) and apigenin(-9.1 kcal/mol) respectively. Molecular dynamics was used to assess the stability of the primary target, KMO, and inhibitor complexes. We found stable interactions of 3′-Hydroxy-ss-naphthoflavone and apigenin with KMO up to 100 ns. Further, kinetic measurements showed that 3′-Hydroxy-alpha-naphthoflavone and 3′-Hydroxy-ss-naphthoflavone induce competitive inhibition with a good IC_{50} activity (15.85 ± 0.98 μM and 18.71 ± 0.78, respectively), while Genkwanin and Apigenin exhibit non-competitive inhibition mechanism (21.61 ± 0.97 μM and 24.14 ± 1.00 μM, respectively).Drug-likeness features and ADME analysis features also showed that the top four compounds could be used as potential candidates to replace the synthetic KMO inhibitor drugs with known side effects and poor brain-blood barrier penetration.

1. Introduction

By converting tryptophan to neuroinflammatory/neurotoxic metabolites, the kynurenine pathway (KP) is critically involved in several neurodegenerative diseases and behavioral disorders [1–4]. As part of this pathway, the enzyme kynurenine-3-monooxygenase

* Corresponding author. Department of Biology, Mohamed Khider University, PO Box 145 RP, Postal code: 07000 Biskra, Algeria.
E-mail addresses: redouane.rebai@univ-biskra.dz, redouane.ralf@gmail.com (R. Rebai).

https://doi.org/10.1016/j.heliyon.2024.e30287
Received 12 February 2024; Received in revised form 31 March 2024; Accepted 23 April 2024
Available online 26 April 2024

(KMO) converts kynurenine (KYN) to 3-hydroxykynurenine (3HK), a free radical generator that causes neuronal cell death and overstimulation of glutamate receptors [3,5]. Compounds that decrease the levels of 3HK, especially KMO inhibitors such as UPF-648

Abbreviations

ADME	absorption distribution metabolism and excretion
BBB	blood-brain-barrier
MD simulations	molecular dynamic simulations
L-Kyn	l-kynurenine
H-bond	hydrogen bond
ns	nanosecond
LD50	Lethal Dose 50
Km	Michaelis constant
Vmax	maximum velocity

(IC50 = 20 nM), KNS366, and GSK 366 (IC50 = 2.3 nM), are being considered for treating several diseases [3,5–11].

Until now, no reports have suggested the inhibitory activity of flavonoids on KMO enzyme using computational tools to discover new inhibitors and drug candidates for neuropsychiatric and neurodegenerative diseases.

The present study determined if natural flavonoid compounds significantly inhibit KMO in molecular simulation and kinetic studies. Flavonoids are part of the polyphenol class of phytonutrients with well-documented biological properties. The polyphenol structure of flavonoids is responsible for their pharmacological activities, including antimicrobial, antiviral, antioxidant, and anti-inflammatory activities [12,13]. They are potent inhibitors of several brain enzymes, including indoleamine 2,3-dioxygenase [14] and monoamine oxidase [15].

We have measured the inhibitory activity of flavonoids on KMO using computational tools to discover new inhibitors and drug candidates for neurodegenerative diseases and behavioral disorders.

2. Materials and methods

2.1. Chemicals and reagents

3′-Hydroxy-alpha-naphthoflavone and 3′-Hydroxy-ss-naphthoflavone were bought from Indofine (Township, NJ, USA), Genkwanin, Apigenin,Ro 61–8048, and DSMOwere obtained from Sigma-Aldrich Co. LLC (Germany). KMO kit and buffers were bought from (Thermo Fisher Scientific (Waltham, MA, USA)).

2.2. Computational method

2.2.1. Receptors preparation

Three-dimensional structures of the protein-ligand complexes were downloaded from the Protein Data Bank (http://www.rcsb.org/). KMO has the PDB code 4J31.

AutoDock Vina was used to perform molecular docking studies. Each protein-ligand complex was prepared by using AutoDock Tools-1.5.6. The first step involves removing water molecules, cofactors, and ligands from the protein's crystal structure. The chain A of the protein was also removed. We added polar hydrogens, and Kollman united atom-type charges to the structure. BIOVIA Discovery Studio Visualizer (2020) was used to picture the docked complexes. Before further analysis, we selected the best position for the ligand to bind to the target protein.

The docking results of the four top-ranked ligands were confirmed by re-docking them into the same defined regions to legitimize the virtual molecular docking protocol for accuracy. The binding scores and protein-ligand interactions were then re-validated using the BINDSURF Achilles blind docking server http://bio-hpc.eu/software/blind-docking-server/. [16].

2.2.2. Ligands preparation

A library of flavonoids was constructed from Sigma-Aldrich's natural product portfolio (https://www.sigmaaldrich.com/DZ/en/products/chemistry-and-biochemicals/biochemicals/natural-products) and was screened using molecular docking.

Before molecular docking, we filtered all compounds using the Lipinski and Veber rules [17,18]; those with reactive functional groups were removed.

Virtual screening results show that apigenin possesses a high binding affinity. Then, compounds structurally similar to apigenin were searched using the Swiss similarity web tool (http://www.swisssimilarity.ch/) [19]. Seventeen flavonoid compounds (Fig. 1), with a score similarity higher than 0.5, were selected and docked to the KMO inhibition site after being drawn by ChemDraw Ultra (version 12.0) optimized using the Avogadro software. We minimized the energies by using the MMFF94 force field.

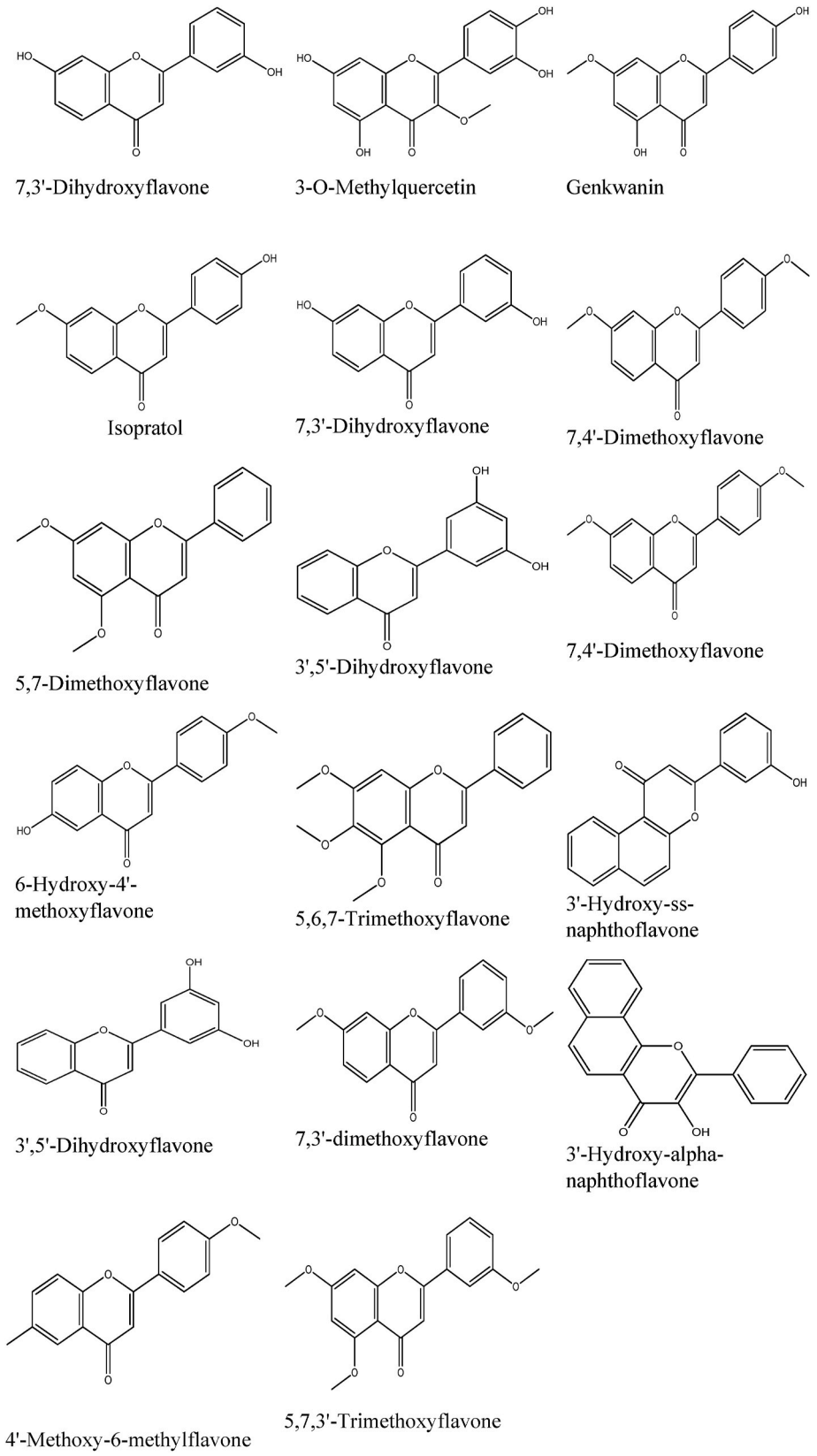

Fig. 1. 2D structures of 17 selected compounds similar to apigenin.

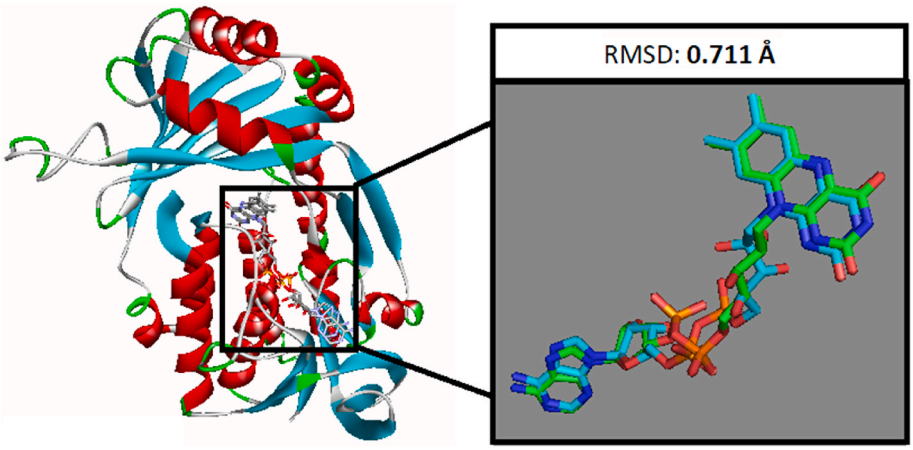

Fig. 2. Validation of docking study; the docked co-crystal ligand and the native ligand with RMSD of 0.711 Å

2.2.3. Drug-likeness and ADMET analysis

We used the SwissADME(http://www.swissadme.ch/) online server to evaluate the pharmacokinetic features such as lipophilicity, gastrointestinal absorption, BBB permeation, and drug-likeness of the best-scored flavonoid compounds [20]. We predicted the physicochemical properties: topological polar surface area, number of hydrogen bond donors, number of hydrogen bond acceptors, and number of rotatable bonds. Additionally, we assessed the toxicity parameters of the selected flavonoids with the ProTox-II web tool (https://tox-new.charite.de/protox_II/).

2.2.4. Molecular dynamic (MD)

We investigated the binding stability of protein-ligand docking complexes using MD, which also offers information on intermolecular interactions within a reference period. We used the Maestro tool System Builder to generate the protein-ligand complex structure of KMO and the top four potential molecules for MD simulations. We immersed the complexes created in a box filled with water molecules via the simple point charge (SPC) scheme. We performed the MD simulations using Maestro-Desmond (Maestro-Desmond Interoperability Tools, Schrödinger, New York, NY, 2020). We set the box size to 10 x 10 × 10 Å. We added sodium and chlorine ions to obtain a final NaCl concentration of 0.15 M. Energy minimization was conducted by 2000 steps using the steepest descent method with a cutoff of 9 Å for van der Waals interactions. We used the Particle Mesh Ewald (PME) method with a tolerance of 10 -9 in the electrostatic part. We did NPT simulations at 300K using the Nosé-Hoover algorithm [21], keeping the pressure at 1 bar using the Martyna-Tobias-Kelinbarostat. The force field OPLS3e was used to do all the runs. The simulation time of each run was 100 ns.

2.3. Enzymatic inhibition assay

We performed the inhibition assay of KMOusingthe method described by Puopolo et al. [22] with a slight modification, using Ro 61–8048 as the positive control. The test molecules were dissolved in 100 mM DMSO and diluted in assay buffer to 1 mM. We incubated in a 96-well plate a reaction made from a mixture of assay buffer (50 μL), human KMO (20 g/mL; 50 μL), test compounds (1 mM; 10 μL), and substrate (40 μL NADPH (10 mM) plus L-kyn (L-Kyn, 20 mM) for 1.5 h at room temperature. All assays were performed in triplicate. The optical densities of each sample were measured on a microplate reader at a wavelength of 340 nm. We determined the enzymatic activity by using the formula below:

$$\% \text{ Activity} = [(\text{Abs}_{\text{sample}} - \text{Abs}_{\text{blank}})/(\text{Abs}_{\text{control}} - \text{Abs}_{\text{blank}})] \times 100$$

The results are reported as the inhibition rate (%) of KMO. A graphical analysis was done to find the IC50 value of each compound.

2.4. Kinetics study

We determined the inhibitory strength of the most potent compounds using the same procedure as the enzyme inhibition assay. We measured the kinetic parameters by creating Lineweaver-Burk plots (double reciprocal plots) using various concentrations of the tested compounds (0 μM–40 μM) with a concentration range of 0–20 μM for the substrate (L-Kyn).

3. Results and discussion

Flavonoids are a broad class of polyphenolic compounds that have neuroprotective properties. They are widely used to prevent cancer, Alzheimer's disease, viral disease, and atherosclerosis. These beneficial effects are attributed to their action on enzymes

Table 1
Molecular docking score of 17 flavonoid phyto-ligands for KMO'sactive site.

Rank	Compound	PubChem CID	Binding Energy (kcal/mol)
1	3′-Hydroxy-alpha-naphthoflavone	13707046	−10.0
2	3′-Hydroxy-ss-naphthoflavone	688843	−9.9
3	Genkwanin	5281617	−9.2
4	Apigenin	5280443	−9.1
5	**Ro 61–8048 (reference inhibitor)**	5282337	−9.1
	3′,5′-Dihydroxyflavone	45933941	−9.0
6	Isopratol	676307	−8.9
7	7,3′-Dihydroxyflavone	5391140	−8.8
8	4′-Methoxy-6-methylflavone	688682	−8.8
9	2,6,7-Trihydroxy-9-methylxanthen-3-one	72721	−8.6
10	3-*O*-Methylquercetin	5280681	−8.6
11	5,7,3′-Trimethoxyflavone	12150586	−8.5
12	7,4′-Dimethoxyflavone	5322058	−8.4
13	7,3′-dimethoxyflavone	688672	−8.4
14	6-Hydroxy-4′-methoxyflavone	688679	−8.4
15	5,7-Dimethoxyflavone	88881	−8.4
16	5,6,7-Trimethoxyflavone	442583	−8.4
17	4′,5-Dimethoxyflavone	688669	−8.2

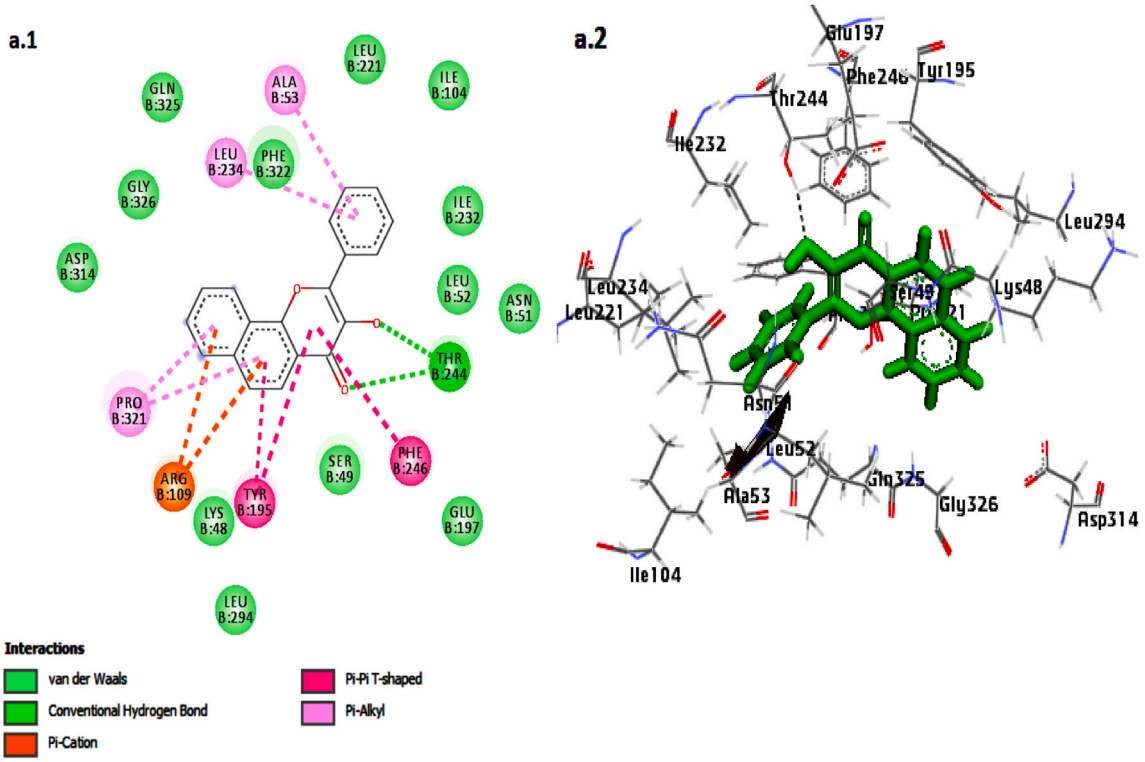

Fig. 3. Interaction of the compounds, 3′-Hydroxy-alpha-naphthoflavone (a1, a2), 3′-Hydroxy-ss-naphthoflavone (b1, b2), genkwanin (c1, c2),apigenin (d1, d2) and Ro 61-8048in the binding site of KMO shown in 3D and 2D representation.

involved in inflammation [23–25]. In this study, we assessed the inhibitory effect of phyto-ligand compounds belonging to the flavonoids on KMO. After validating the docking procedure, we did a structure-based virtual screening of the co-crystal ligand by evaluating the analogy between the lowest energy state predicted by AutoDock Vina and the binding mode of the native ligand (Fig. 2). The root mean square deviation (RMSD) value after the docking procedure was 0.711 Å, which is within the desired range (i.e., less than 2.0 Å).

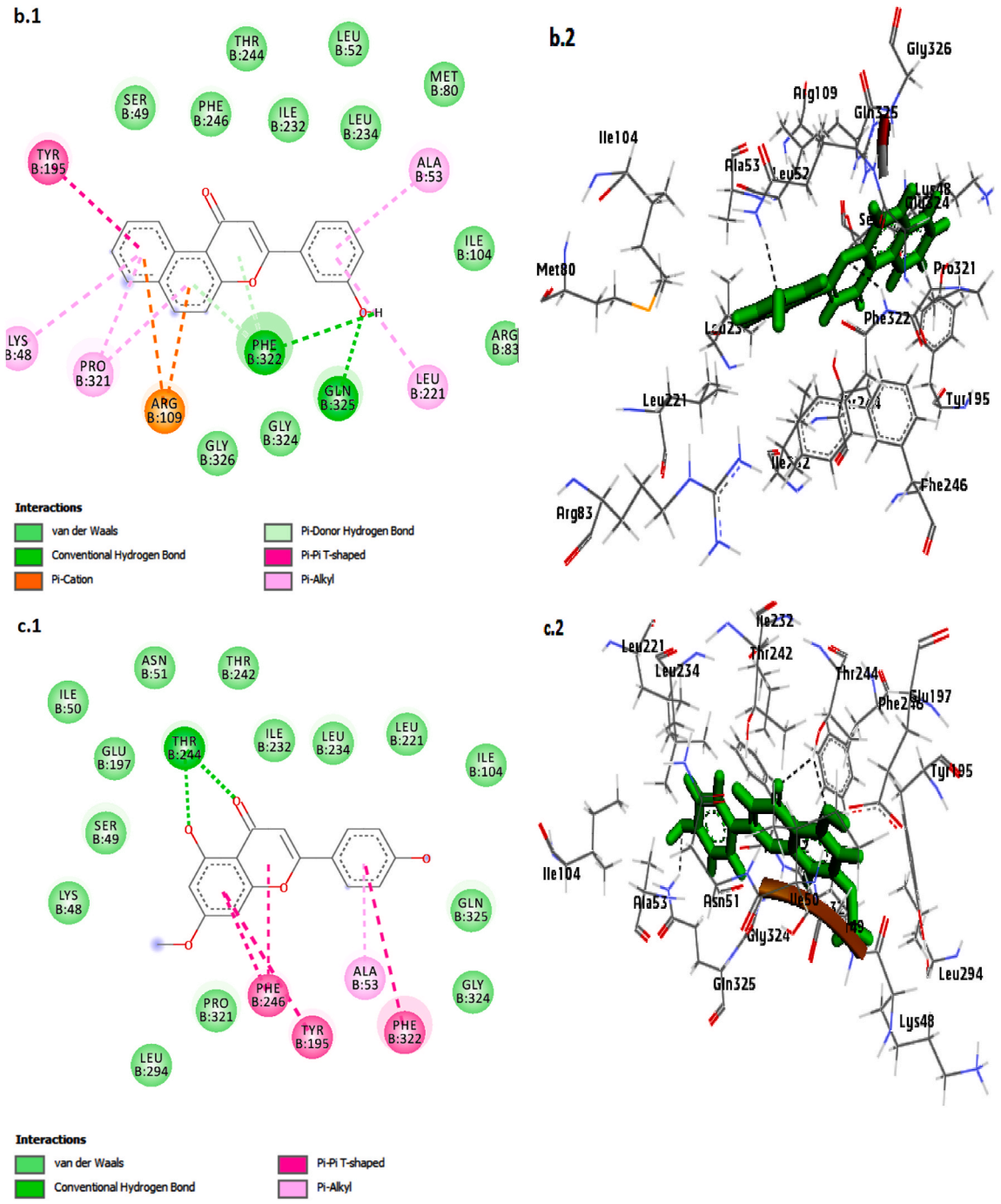

Fig. 3. (*continued*).

3.1. Computational method

3.1.1. Molecular docking

In the present study, 17 flavonoids, similar to apigenin, were identified from the Swiss Similarity server. These phytochemicals were docked in the binding site of the KMO enzyme.

Table 1 lists the docking scores of the studied compounds. The top four compounds in terms of affinity (Fig. 3)are 3′-Hydroxy-alpha-naphthoflavone, which exhibited the lowest docking score (−10.0 kcal/mol), followed by 3′-Hydroxy-ss-naphthoflavone (−9.9 kcal/mol), genkwanin (−9.2 kcal/mol) and apigenin (−9.1 kcal/mol), respectively. Interestingly, these flavonoid ligands showedhigher

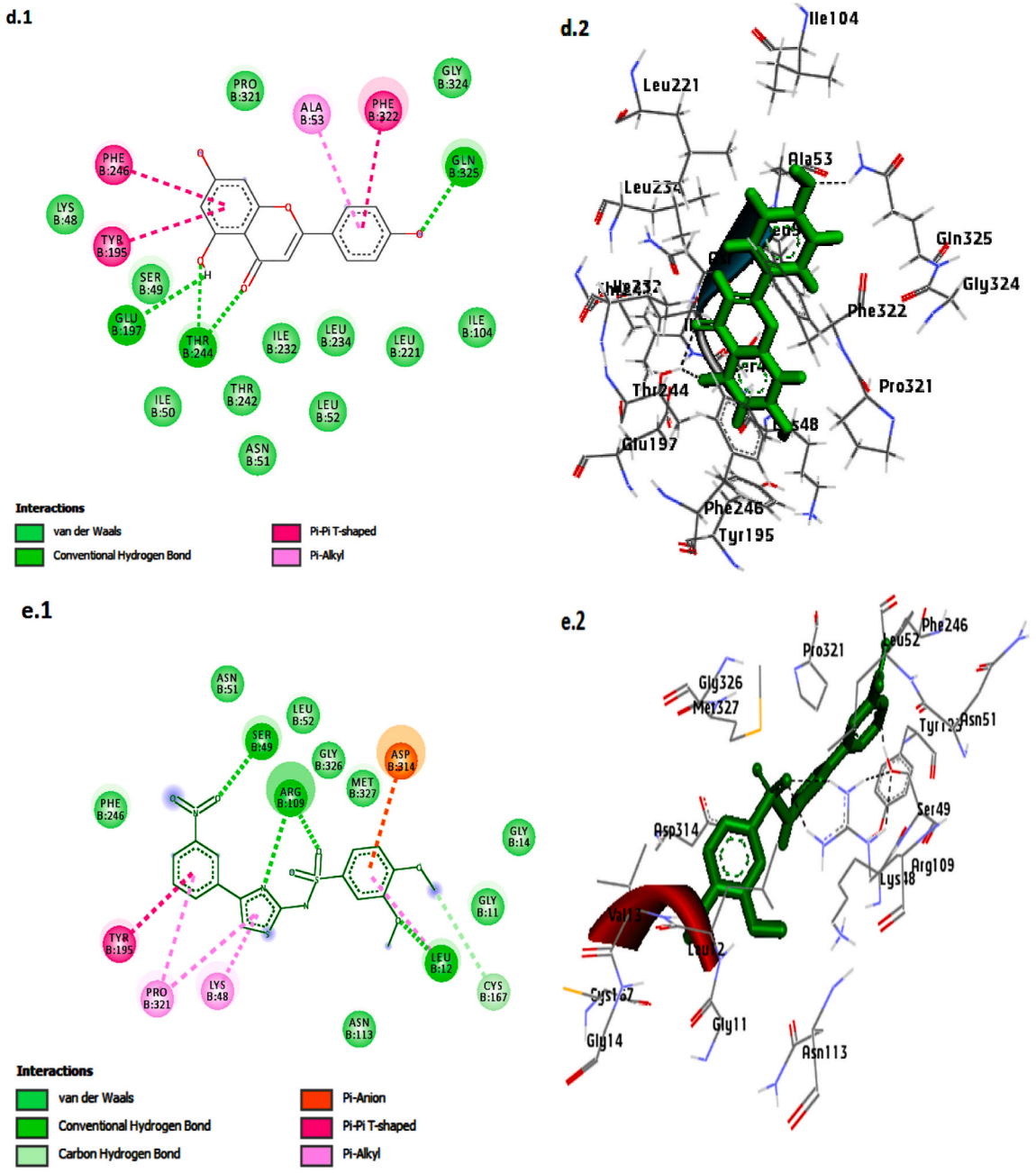

Fig. 3. (*continued*).

docking scores for KMO thanthe reference inhibitor, Ro 61–8048, which scored −9.1 kcal/mol.

Molecular docking analysis revealed several molecular interactions, notably H-bonds and hydrophobic interactions between the ligand molecules and the target enzyme active site residues.Furthermore, the binding poses of the lead KMO inhibitors and standard compounds are depicted in Figs. 3 and 4.

Arg 109, Ser 49, and Leu 12 residues were involved in hydrogen bond formation with Ro 61–8048. Besides, the amino acids Lys 48, Asn 51, Leu 52, Asn 113, Cyt 167, Tyr 195 Phe 246, Pro 321, Gly 326, and Met 327 were involved inVan der Waals andhydrophobic interactions.

The lead compound, 3′-Hydroxy-alpha-naphthoflavone,exhibited a combination of hydrogen bonding, van der Waals, hydrophobic interactions, π–π T-shaped, and π-Alkyl interaction in the docked complex. It formed two hydrogen bonds with Thr 244 amino acid residue, a π-cation bond with Arg 109, π-Alkyl interaction with residues Ala 53, Leu 234, and Pro 231, and two π–π T-shaped bonds with Tyr 195 andPhe 246 residues (Fig. 3; a1, a2).

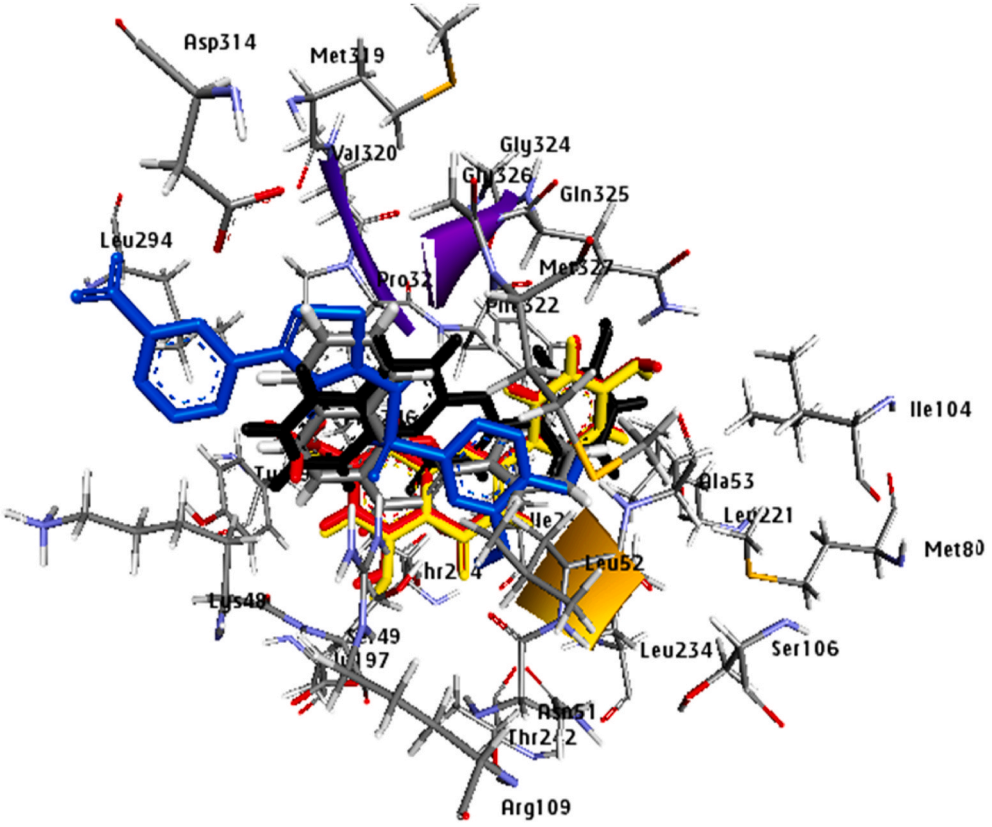

Fig. 4. Interaction and binding pose of the four lead compounds and reference inhibitor (Ro 61–8048)in the active site; 3′-Hydroxy-alpha-naphthoflavone (Grey), 3′-Hydroxy-ss-naphthoflavone (Black), Genkwanin(Red), Apigenin (Yalow) and Ro 61–8048 (Blue).

Table 2
Drug-likeness and ADME proprieties of the lead compounds.

Compound	MW g/mol	AccptHB	DonorHB	Nrot	TPSA (Å^2)	LogP< 5	GI absorption	BBB permeability	Bioavailability score
3′-Hydroxy-alpha-naphthoflavone	288.30	3	1	1	50.44	4.32	High	Yes	0.55
3′-Hydroxy-ss-naphthoflavone	288.30	3	1	1	50.44	4.32	High	Yes	0.55
Genkwanin	284.26	5	2	2	79.90	2.88	High	No	0.55
Apigenin	270.24	5	3	1	90.90	2.58	High	No	0.55
Ro 61-8048	421.45	7	1	7	159.96	4.43	Low	No	0.55

MW: molecular weight; AccptHB: acceptor hydrogen bond; DonorHB: donor H-bond; Nrot:Rotatable Bond; TPSA: Topological Polar Surface Area; Log $P_{o/w}$: lipophilicity octanol/water; GI: Gastrointestinal absorption.

In addition, 3′-Hydroxy-ss-naphthoflavone formed two conventional hydrogen bonds with Gln, 325 andPhe 322 residues, two π-donor hydrogen bonds with the Phe 322 residue, two π-Cation with Arg 109, four π-Alkyl interactions with Lys 48, Ala 53, Leu 221, and Pro 321 residues, and made one π–π T-shaped bond with Tyr 195 amino acid residue (Fig. 3; b.1, b2).

Furthermore, the bonding of genkwanin with the active site of KMO involves various intriguing interactions: two hydrogen bonds with Thr 244 residue, π-Sigma bound with Ile 232 residue, three Pi-Pi-T-shaped bonds with Tyr 195, Phe 246, and Phe 322 residues, and three Pi-Alkyl interactions with Lys 48, Ala 53, and Pro 321 amino acids residues.

We found almost identical interactions between apigenin and the KMO receptor (Fig. 3; d1, d2). Apigenin formed four hydrogen bonds, two each with Thr 244, Glu 197, Gln 325, one with Pi-Sigma (Ile 232), one π-Alkyl with Ala 53 residue, and three π–π T-shaped bonds with Tyr 195, Phe 246, and Phe 322 amino acid residues.

3.1.2. Drug-likeness proprieties and ADMET analysis

The pharmacokinetics and properties of the selected compounds are summarized in Table 2. We determined the drug-likeness using the *in silico* SwissADME server to test for Lipinski's rule of five parameters, including lipophilicity, the number of H-bond donors and

Table 3
Toxicity parameters prediction of the lead compounds.

Parameters		3′-Hydroxy-alpha-naphthoflavone	3′-Hydroxy-ss-naphthoflavone	Genkwanin	Apigenin	Ro 61-8048
LD_{50}(mg/kg)		2500	4000	3919	2500	4500
Prediction class		Class V	Class V	Class V	Class V	Class V
Hepatotoxicity	Prediction	Inactive	Inactive	Inactive	Inactive	Active
	Probability	0.65	0.63	0.72	0.68	0.61
Carcinogenicity	Prediction	Inactive	Active	Active	Inactive	Active
	Probability	0.50	0.56	0.51	0.62	0.56
Immunotoxicity	Prediction	Inactive	Inactive	Inactive	Inactive	Inactive
	Probability	0.94	0.85	0.95	0.99	0.98
Mutagenicity	Prediction	Inactive	Inactive	Active	Inactive	Active
	Probability	0.60	0.62	0.57	0.57	0.52
Prediction accuracy		69.26 %	70.97 %	70.97 %	70.97 %	67.38 %

acceptors, and the molecular weight.

The results show that the four top flavonoids similar to apigenin (listed in Table 1) do not violate Lipinski and Veber rules (Table 2); they will be good candidates as orally active drugs.

Blood-brain barrier permeability (BBB) for 3′-Hydroxy-alpha-naphthoflavone and 3′-Hydroxy-ss-naphthoflavone was higher, as well as the gastrointestinal absorption for the four compounds (Table 2).The lead compounds with the highest affinity for KMO exhibited enough lipophilicity level (logP) to suggest that they diffuse through the cell membrane.

Furthermore, the Ld_{50} value, toxicity class, hepatotoxicity, carcinogenicity, immunotoxicity, and mutagenicity of the four top compounds have been analyzed on the ProTox-II web server results (Table 3).3′-Hydroxy-ss-naphthoflavone and genkwanin exhibited the highest LD_{50} value of 4000 mg/kg and 3919 mg/kg, respectively, followed by 3′-Hydroxy-alpha-naphthoflavone and apigenin with LD_{50} of 2500 mg/kg, respectively. These compounds belong to the same class (Class V) and are found to be inactive for hepatotoxicity and immunotoxicity, except for 3′-Hydroxy-ss-naphthoflavone and genkwanin, which are active for carcinogenicity.

3.1.3. Molecular dynamic (MD)

An MD study of the top four docked complexes at 100 ns was conducted to assessthe stability of ligand-KMO complexes. We evaluated the MD simulations using the root mean square deviation (RMSD), root mean square fluctuation (RMSF), and protein-ligand interactions. The RMSD is used to assess the conformational stability of a structure during simulation by evaluating the average change in atom displacement relative to a reference.

The RMSD graph (Fig. 5, A1) of the KMO-3′-Hydroxy-alpha-naphthoflavone complex shows a slight fluctuation, less than 3 Å during the first 60 ns of MD simulation, then the complex ligand-protein shows significant stability. However, it was slightly divergent after 60 ns of simulation, within the acceptable range of 0–3 Å. The RMSD plot of the KMO-3′-Hydroxy-ss-naphthoflavone complex in Fig. 5, B1 shows that the complex is stable throughout the simulation period except for a slight deviation between 40 and 60 ns. The RMSD plot of (Fig. 5, C1) shows that the KMO- genkwanin complex was unstable at the beginning of the simulation; there was high fluctuation from 0 to 10 ns of simulation, and after 10 ns, it became stable up to 80 ns. Although a slight deviation was seen between 80 and 90 ns, the complexes stabilized at the end of the simulation. The KMO-apigenin complex plot (Fig. 5, D1) shows good stability from the simulation's start to end. We observed only a slight fluctuation between 90 and 95 ns, indicating that the complex has not undergone significant conformational changes.

We performed RMSF analyses to assess the flexibility per residue using the docked complex structures. The N and C terminals of A2, B2, C2, and D2 fluctuate more than other regions of the protein (Fig. 5). Peaks indicate protein fluctuations; the lower the associated fluctuations, the more stable the complexes during simulation, showing that the system is in equilibrium [26].The RMSF did not vary much over the 100 ns simulation period, and the average RMSF values were kept constant for all complexes except for the higher RMSF seen in the 3′-Hydroxy-alpha-naphthoflavone-KMO and 3′-Hydroxy-ss-naphthoflavone-KMO complexes, at the backbone residue positions between Gly81 and Tyr96.

3.2. KMO inhibitory activity

All flavonoid compounds displayed a good inhibitory potential of KMO, with IC50 values varying between 15.85 ± 0.98 μM and 24.14 ± 1.00 μM at concentrations ranging from 2.5 to 40 μM. Among the flavonoid compounds, 3′-Hydroxy-alpha-naphthoflavone was identified as the lead compound with the highest IC50 activity (15.85 ± 0.98 μM), while apigenin (IC50 value 24.14 ± 1.00 μM) showed the least inhibitory effect. However, Ro 61–8048 (IC50 value 4.91 ± 0.31 μM) was the most effective KMO inhibitor (Table 4).

3.3. Inhibition mechanisms of KMO

The kinetics of the tested flavonoids were quantitatively analyzed using Lineweaver-Burk plots to investigate the type of inhibition. As noted in (Fig. 6, A, and Fig. 6, B), the value of Km increased without changing Vmax in the presence of increasing concentrations of the inhibitors. In addition, the y-intercept of the curves was unaffected as the concentration of the compounds increased, while the

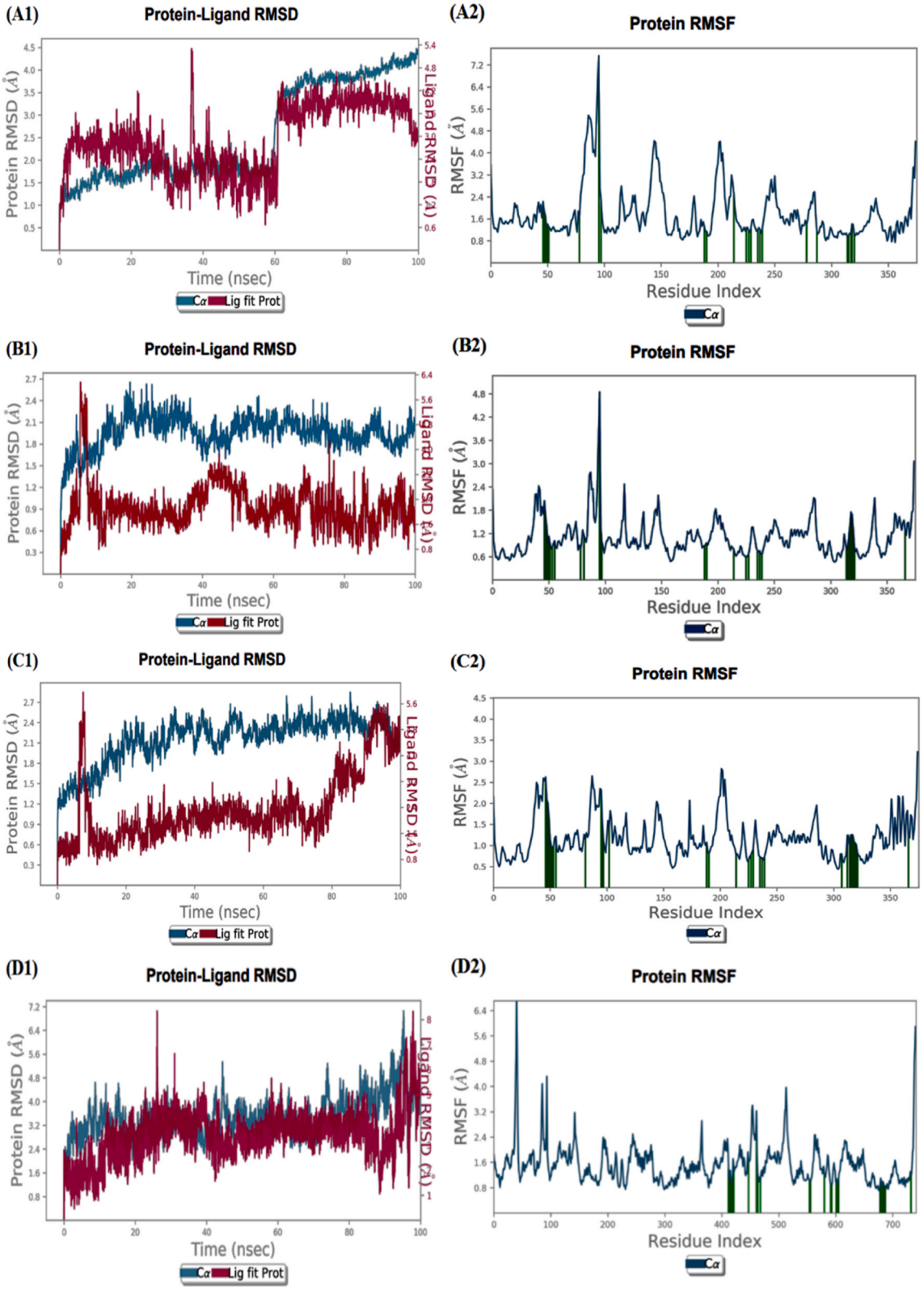

(caption on next page)

Fig. 5. MD for the 4 top KMO-complexes, (A1): RMSD plot of the KMO-3′-Hydroxy-alpha-naphthoflavone, (A2): RMSF plot of KMO-3′-Hydroxy-alpha-naphthoflavone complex, (B1): RMSD plot of KMO-3′-Hydroxy-ss-naphthoflavone, (B2): RMSF plot of KMO-3′-Hydroxy-ss-naphthoflavone complex. (C1): RMSD plot of KMO-genkwanin complex, (C2) RMSF plot of KMO-genkwanin complex. (D1): RMSD plot of KMO-apigenin complex, (D2): RMSF plot of KMO-apigenin complex.

Table 4
KMO inhibition (IC_{50}) by the lead compounds.

Compound	IC_{50} (μM)	Inhibition type
3′-Hydroxy-alpha-naphthoflavone	15.85 ± 0.98	Competitive
3′-Hydroxy-ss-naphthoflavone	18.71 ± 0.78	Competitive
Genkwanin	21.61 ± 0.97	Non-competitive
Apigenin	24.14 ± 1.00	Non-competitive
Ro 61–8048 (positive control)	4.96 ± 0.31	NT (not tested)

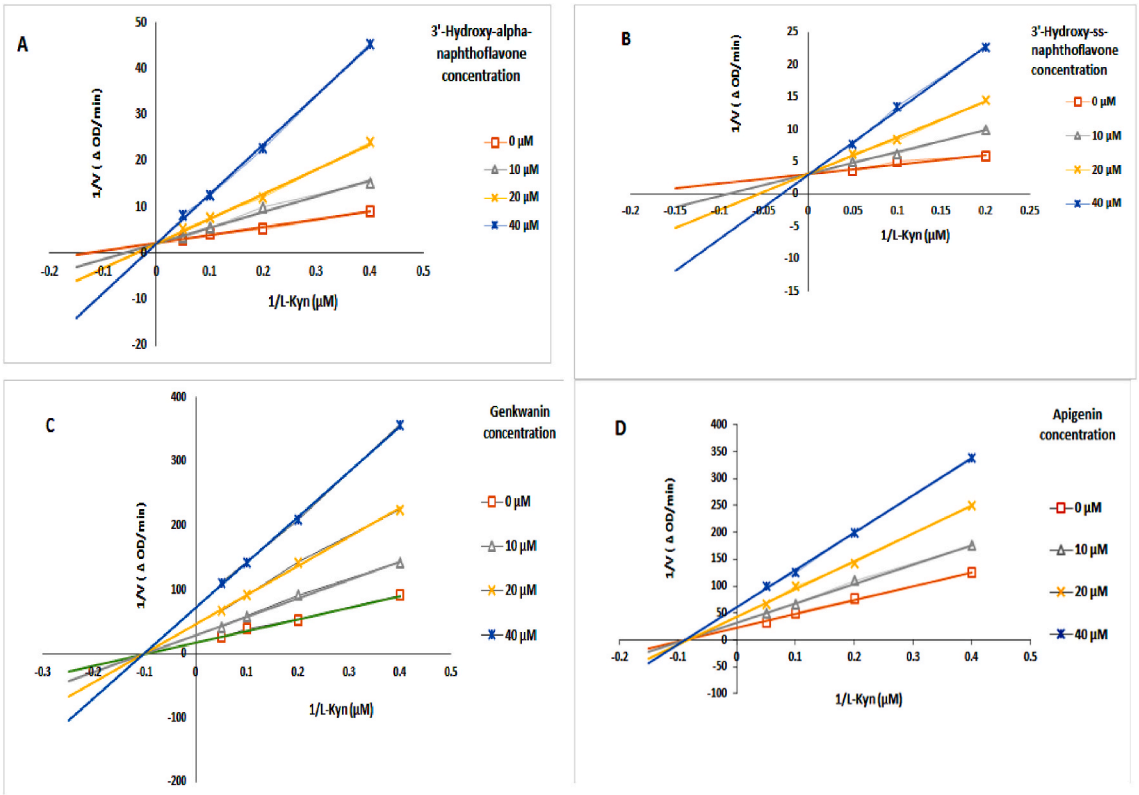

Fig. 6. Inhibitory kinetics of flavonoids (3′-Hydroxy-alpha-naphthoflavone, 3′-Hydroxy-ss-naphthoflavone, genkwanin, and apigenin). KMO enzyme was treated with 0–40 μM of each compound using 0–20 μM of L-Kyn as the substrate. Experiments were performed in triplicate and repeated three times with similar results.

addition of inhibitors changed the x-intercept. This behavior shows that 3′-hydroxy-alpha-naphthoflavone and 3′-hydroxy-ss-naphthoflavone are competitive inhibitors.

In Fig. 6C and D, the y-intercept changed by adding inhibitors, but there was no effect on the x-intercept, showing that the Vmax values decreased, and the Km values remained constant. We conclude that genkwanin and apigenin are non-competitive inhibitors.

The studied compounds exhibit a strong affinity and effectively engage with the critical residues located within the inhibitor binding site of the protein, demonstrating a remarkable stability within the binding pocket without unnecessary fluctuations. These findings suggest that the selected compounds have the ability to trigger biological reactions within the KMO enzyme, demonstrating their promising inhibitory effects to enhance specific activities within the biological system.

4. Conclusion

Four potent KMO inhibitors from Sigma-Aldrich chemical library of natural compounds were identified based on docking score, predicted binding energies, and *in vitro* validation by establishing IC 50s. The four compounds exhibited favorable pharmacokinetic proprieties and acceptable RMSD and RMSF stability. The results presented here could help select a lead molecule for future *in vivo* research, drug discovery, and development targeting KMO.

Funding

This work was supported by the University of Mohamed Khider, Biskra, Algeria (RedouaneRebai and Abdennacer Boudah). Funding was also obtained from the Painless Research Foundation (Redouane Rebai, Luc Jasmin, Abdennacer Boudah). Funding sources were not involved in conducting the research and preparing the article.

Institutional review Board statement

Not applicable.

Informed consent statement

Not applicable.

Data availability

Data will be made available on request.

CRediT authorship contribution statement

Redouane Rebai: Writing – review & editing, Writing – original draft, Visualization, Software, Investigation, Formal analysis, Conceptualization. **Miguel Carmena-Bargueño:** Writing – original draft, Validation, Software, Methodology. **Mohammed Esseddik Toumi:** Validation, Software, Methodology. **Imene Derardja:** Visualization, Validation, Software, Methodology. **Luc Jasmin:** Writing – review & editing, Validation, Supervision, Conceptualization. **Horacio Pérez-Sánchez:** Writing – review & editing, Writing – original draft, Validation, Supervision. **Abdennacer Boudah:** Writing – review & editing, Writing – original draft, Validation, Supervision, Conceptualization.

Declaration of competing interest

The authors declare that they have no known competing financial interests or personal relationships that could have appeared to influence the work reported in this paper.

References

[1] B. Hahn, C.H. Reneski, A. Pocivavsek, R. Schwarcz, Prenatal kynurenine treatment in rats causes schizophrenia-like broad monitoring deficits in adulthood, Psychopharmacol. 235 (3) (2018) 651–661, https://doi.org/10.1007/s00213-017-4780-9.
[2] J. Kindler, C.K. Lim, C.S. Weickert, D. Boerrigter, C. Galletly, D. Liu, K.R. Jacobs, R. Balzan, J. Bruggemann, M. O'Donnell, R. Lenroot, G.J. Guillemin, T. W. Weickert, Dysregulation of kynurenine metabolism is related to proinflammatory cytokines, attention, and prefrontal cortex volume in schizophrenia, Mol. Psychiatry 25 (11) (2020) 2860–2872, https://doi.org/10.1038/s41380-019-0401-9.
[3] J. Savitz, The kynurenine pathway: a finger in every pie, Mol. Psychiatry 25 (1) (2020) 131–147, https://doi.org/10.1038/s41380-019-0414-4.
[4] J.R. Smith, J.F. Jamie, G.J. Guillemin, G. J. Kynurenine-3-monooxygenase: a review of structure, mechanism, and inhibitors, Drug Discov. Today 21 (2) (2016) 315–324, https://doi.org/10.1016/j.drudis.2015.11.001.
[5] S. Zhang, M. Sakuma, G.S. Deora, C.W. Levy, A. Klausing, C. Breda, K.D. Read, C.D. Edlin, B.P. Ross, M.W. Muelas, P.J. Day, S. O'Hagan, D.B. Kell, R. Scharcz, D. Leys, D.J. Heyes, F. Giorgini, N.S. Scrutton, A brain-permeable inhibitor of the neurodegenerative disease target kynurenine 3-monooxygenase prevents accumulation of neurotoxic metabolites, Commun. Biol. 2 (1) (2019) 271, https://doi.org/10.1038/s42003-019-0520-5.
[6] M.Y. Bai, D.B. Lovejoy, G.J. Guillemin, R. Kozak, T.W. Stone, M.M. Koola, M.M. Galantamine-Memantine, Combination and kynurenine pathway enzyme inhibitors in the treatment of neuropsychiatric disorders, Complex Psychiatry 7 (1–2) (2021) 19–33, https://doi.org/10.1159/000515066.
[7] J.P. Hutchinson, P. Rowland, M.R. Taylor, E.M. Christodoulou, C. Haslam, C.I. Hobbs, D.S. Holmes, P. Homes, J. Lidlle, D.J. Mole, L. Uings, A.L. Walker, S. P. Webster, C.G. Mowat, C.W. Chung, Structural and mechanistic basis of differentiated inhibitors of the acute pancreatitis target kynurenine-3-monooxygenase, Nat. Commun. 8 (1) (2017) 1–12, https://doi.org/10.1038/ncomms15827, 2017.
[8] A. Noorbakhsh, K.E. Hosseininezhadian, C. Farshadfar, N. Ardalan, Designing a natural inhibitor against human kynurenine aminotransferase type II and a comparison with PF-04859989: a computational effort against schizophrenia, J. Biomol. Struct. Dyn. (2021) 1–14, https://doi.org/10.1080/07391102.2021.1893817.
[9] A. Pocivavsek, G.I. Elmer, R. Schwarcz, Inhibition of kynurenine aminotransferase II attenuates hippocampus-dependent memory deficit in adult rats treated prenatally with kynurenine, Hippocampus 29 (2) (2019) 73–77, https://doi.org/10.1002/hipo.23040.
[10] M.T. Sapko, P. Guidetti, P. Yu, D.A. Tagle, R. Pellicciari, R. Schwarcz, Endogenous kynurenate controls the vulnerability of striatal neurons to quinolinate: implications for Huntington's disease, Exp. Neurol. 197 (1) (2006) 31–40, https://doi.org/10.1016/j.expneurol.2005.07.004, 2006.
[11] D. Zwilling, S.Y. Huang, K.V. Sathyasaikumar, F.M. Notarangelo, P. Guidetti, H.Q. Wu, P.J. Muchowski, Kynurenine 3-monooxygenase inhibition in blood ameliorates neurodegeneration, Cell 145 (6) (2011) 863–874, https://doi.org/10.1016/j.cell.2011.05.020.

[12] S.A. Cherrak, H. Merzouk, N. Mokhtari-Soulimane, Potential bioactive glycosylated flavonoids as SARS-CoV-2 main protease inhibitors: a molecular docking and simulation studies, PLoS One 15 (10) (2020) e0240653, https://doi.org/10.1371/journal.pone.024065.
[13] M.C. Dias, D.C. Pinto, A. Silva, Plant flavonoids: chemical characteristics and biological activity, Molecules 26 (17) (2021) 5377, https://doi.org/10.3390/molecules26175377.
[14] M. Kwon, S.K. Ko, M. Jang, G.H. Kim, I.J. Ryoo, S. Son, J.S. Ahn, Inhibitory effects of flavonoids isolated from Sophora flavescens on indoleamine 2, 3-dioxygenase 1 activity, J Enzyme Inhib Med Chem 34 (1) (2019) 1481–1488, https://doi.org/10.1080/14756366.2019.1640218.
[15] A.N. Esfahani, M. Mirzaei, Flavonoid derivatives for monoamine oxidase–A inhibition, Adv. J. Chem. B 1 (1) (2019) 17–22, https://doi.org/10.33945/SAMI/AJCB.2019.1.4, 2019.
[16] I. Sánchez-Linares, H. Pérez-Sánchez, J.M. Cecilia, J.M. García, High-throughput parallel blind virtual screening using BINDSURF, BMC Bioinf. 13 (14) (2012) 1–14, https://doi.org/10.1186/1471-2105-13-S14-S13.
[17] C.A. Lipinski, Drug-like properties and the causes of poor solubility and poor permeability, J. Pharmacol. Toxicol. Methods 44 (1) (2000) 235–249, https://doi.org/10.1016/S1056-8719(00)00107-6.
[18] D.F. Veber, S.R. Johnson, H.Y. Cheng, B.R. Smith, K.W. Ward, K.D. Kopple, Molecular properties that influence the oral bioavailability of drug candidates, J. Med. Chem. 45 (12) (2002) 2615–2623, https://doi.org/10.1021/jm020017n.
[19] V. Zoete, A. Daina, C. Bovigny, O. Michielin, SwissSimilarity: a web tool for low to ultra high throughput ligand-based virtual screening, J. Chem. Inf. Model. 56 (8) (2016) 1399–1404, https://doi.org/10.1021/acs.jcim.6b00174.
[20] A. Daina, O. Michielin, V. Zoete, SwissADME: a free web tool to evaluate pharmacokinetics, drug-likeness and medicinal chemistry friendliness of small molecules, Sci. Rep. 7 (2017) 42717, https://doi.org/10.1038/srep42717.
[21] S. Nosé, A unified formulation of the constant temperature molecular dynamics methods, J. Chem. Phys. 81 (1) (1984) 511–519, https://doi.org/10.1063/1.447334.
[22] T. Puopolo, T. Chang, C. Liu, H. Li, X. Liu, X. Wu, H. Ma, N.P. Seeram, Gram-scale preparation of cannflavin A from hemp (Cannabis sativa L.) and its inhibitory effect on tryptophan catabolism enzyme kynurenine-3-monooxygenase, Biology 11 (10) (2022) 1416, https://doi.org/10.3390/biology11101416.
[23] J. Bernardo, I. Malheiro, R.A. Videira, P. Valentão, A.C. Santos, F. Veiga, P.B. Andrade, Trichiliacatigua and Turneradiffusa extracts: in vitro inhibition of tyrosinase, antiglycation activity and effects on enzymes and pathways engaged in the neuroinflammatory process, J. Ethnopharmacol. 271 (2021) 113865, https://doi.org/10.1016/j.jep.2021.113865.
[24] A.M.A. Hamsalakshmi, M. ArehallyMarappa, S. Joghee, S.B. Chidambaram, Therapeutic benefits of flavonoids against neuroinflammation: a systematic review, Inflammopharmacology (2022) 1–26, https://doi.org/10.1007/s10787-021-00895-8.
[25] V.V. Mossine, J.K. Waters, Z. Gu, G.Y. Sun, T.P. Mawhinney, Bidirectional responses of eight neuroinflammation-related transcriptional factors to 64 flavonoids in astrocytes with transposable insulated signaling pathway reporters, ACS Chem. Neurosci. 13 (5) (2022) 613–623, https://doi.org/10.1021/acschemneuro.1c00750.
[26] S. Akbar, S. Das, A. Iqubal, B. Ahmed, Synthesis, biological evaluation and molecular dynamics studies of oxadiazine derivatives as potential anti-hepatotoxic agents, J. Biomol. Struct. Dyn. 40 (20) (2022) 9974–9991, https://doi.org/10.1080/07391102.2021.1938233.